(13) M. Sandström and I. Persson, *Acta Chem. Scand., Ser. A*, **32**, 95 (1978).
(14) G. Kopfmann and R. Huber, *Acta Crystallogr., Sect. A*, **24**, 348 (1968); A. C. T. North, D. C. Phillips, and F. Scott Mathews, *ibid.*, 351 (1968).
(15) Supplementary material.
(16) R. J. Williams, A. C. Larson, and D. T. Cromer, *Acta Crystallogr., Sect. B*, **28**, 858 (1972).
(17) E. Luukkonen, A. Pajunen, et al., *Suom. Kemistil. B*, **42**, 474, 348 (1969); **43**, 160 (1970).
(18) R. V. Chastain, Jr., and T. L. Dominick, *Inorg. Chem.*, **12**, 2621 (1973).
(19) M. Cannas, G. Carta, and G. Marongiu, *J. Chem. Soc., Dalton Trans.*, 251 (1973).
(20) J. Korvenranta and A. Pajunen, *Suom. Kemistil. B*, **43**, 119 (1970).
(21) R. Hämäläinen and A. Pajunen, *Suom. Kemistil. B*, **45**, 117, 122 (1972); *Finn. Chem. Lett.*, 150 (1974).
(22) R. Hämäläinen, *Suom. Kemistil. B*, **44**, 89 (1971); **46**, 237 (1973).
(23) P. J. M. W. L. Birker, P. T. Crisp, and C. J. Moore, *Acta Crystallogr., Sect. B*, **33**, 3194 (1977).
(24) M. A. Bush and D. E. Fenton, *J. Chem. Soc. A*, 2446 (1971).
(25) A. Pajunen, E. Näsäkkälä, and S. Pajunen, *Cryst. Struct. Commun.*, **7**, 63 (1978).
(26) A. Pajunen, K. Smolander, and I. Belinskij, *Suom. Kmistil. B*, **45**, 317 (1972).

Contribution from the Department of Chemistry, University of Virginia, Charlottesville, Virginia 22901

High- and Low-Spin Interconversion in a Series of (α-Picolylamine)iron(II) Complexes

ANTHONY M. GREENAWAY, CHARLES J. O'CONNOR, ALAN SCHROCK, and EKK SINN*

Received March 27, 1979

The magnetic properties of $[Fe(\alpha\text{-P})_3]Br_2\cdot S$ (α-P = α-picolylamine; S = methanol, ethanol) and $[Fe(\alpha\text{-P})_3]Cl_2\cdot C_2H_5OH$ and the crystal structure of the latter complex have been determined. Each of the complexes is high spin at room temperature and each undergoes a similar transition to low spin in the region 130–90 K. In each case the transition is relatively sharp, being mostly complete in the region 130–110 K, and is sharper than in the analogous complex $[Fe(\alpha\text{-P})_3]Cl_2\cdot CH_3OH$. We noted earlier that $[Fe(\alpha\text{-P})_3]^{2+}$ has approximate threefold symmetry in the purely low-spin $[Fe(\alpha\text{-P})_3]Cl_2\cdot 2H_2O$ (*fac* geometry) but has one of its ligands coordinated with the two donor atoms reversed in $[Fe(\alpha\text{-P})_3]Cl_2\cdot CH_3OH$ (*mer* geometry). The crystal structure of $[Fe(\alpha\text{-P})_3]Cl_2\cdot C_2H_5OH$ and the similarity of the magnetic properties indicate that the present complexes all have the same "ligand-reversed" structure of the $[Fe(\alpha\text{-P})_3]^{2+}$ ion. Removal of the included solvent S drastically alters the magnetic properties, eliminating the sharp spin transition and replacing it with a spin equilibrium which is so gradual that low spin ($^1A_1$) is not attained even at the lowest temperatures studied (4 K). Literature observations of such very gradual spin transitions can now be explained in terms of sample drying which removed solvent that had originally been held in the lattice via hydrogen bonding. The crystal structure of $[Fe(\alpha\text{-P})_3]Cl_2\cdot C_2H_5OH$ reveals hydrogen bonding between the ethanol molecule and a halogen but not with the cation. Comparison of this structure with that of $[Fe(\alpha\text{-P})_3]Cl_2\cdot 2H_2O$ reveals a large change, 0.18 Å, in the average metal–ligand bond length between the high-spin and low-spin iron(II) species, providing important support for our previous determination of 0.19 Å for this quantity. Crystal data for $[Fe(\alpha\text{-P})_3]Cl_2\cdot C_2H_5OH$: space group $P2_1/c$, $Z = 4$, $a = 10.937$ (5) Å, $b = 22.061$ (9) Å, $c = 11.571$ (6) Å, $\beta = 116.70$ (4)°, $V = 2496$ Å^3, $R = 5.3\%$ for 1470 reflections.

Introduction

Complexes lying near the high-spin–low-spin crossover have been shown to be very sensitive to changes in temperature and pressure, minor chemical changes in the ligands, counteranions in the case of cationic complexes, and solvent molecules incorporated in the lattice.[1-12] Quite dramatic solvent effects have been demonstrated in ferric dithiocarbamates,[5-8] in the iron(III) complexes of B_2trien (B = salicylaldehyde, acetylacetone, 3-chloroacetylacetone)[9,10] and in the iron(II) complexes $[Fe(\alpha\text{-P})_3]Cl_2$ (α-P = α-picolylamine).[12] In the complexes $[Fe(B_2trien)]^+X^-$ (where X = Cl, NO_3), inclusion of water molecules, simultaneously hydrogen bonded to both the cation and the anion, induces a low-spin state, while analogous anhydrous complexes tend to be pure high spin or to exhibit a high-spin–low-spin equilibrium.[9,10] Similarly, the water molecules in the low-spin $[Fe(\alpha\text{-P})_3]Cl_2\cdot 2H_2O$ (*fac* structure A, Figure 1) are hydrogen bonded to both the cations and the anions, while there is no link between the methanol and the cations in $[Fe(\alpha\text{-P})_3]Cl_2\cdot CH_3OH$ (*mer* structure B, Figure 1), which exhibits a high-spin–low-spin equilibrium.[11] We show here that occluded solvent molecules in $[Fe(\alpha\text{-P})_3]Cl_2\cdot C_2H_5OH$, which also exhibits the spin equilibrium, are likewise isolated from the cations. Whether the magnetic differences are induced directly by the solvent molecules or indirectly by inducing structural differences or both is now an important question. We present evidence which suggests that, while solvent–cation contact is important if only by reducing the amount of anion–cation contact, the cation structures A and B are magnetically different, the more distorted B tending to have the weaker crystal field (closer to high spin). Inclusion of hydrogen-bonding solvents, such as chloroform, dichloromethane, or water, in ferric dithiocarbamate lattices tends to shift the spin-state equilibrium toward the high-spin side and to lower the energy of the intermediate $S = {}^3/_2$ spin state.[5-8] Similarly, the high residual magnetic moment at low temperatures reported[13] for $[Fe(\alpha\text{-P})_3]Br_2$ but not for $[Fe(\alpha\text{-P})_3]Cl_2$ raises the question of a low-lying intermediate spin state ($S = 1$) for the bromide complex. We show here that no low-lying intermediate spin state exists in $[Fe(\alpha\text{-P})_3]Br_2\cdot S$ (S = CH_3OH, C_2H_5OH), but that a spin-state crossover involving $S = 0$ ($^1A_1$) and $S = 2$ ($^5T_2$) states exists in each of the complexes $[Fe(\alpha\text{-P})_3]X_2\cdot S$ (X = Cl, Br; S = CH_3OH, C_2H_5OH). A magnetic study of an ethanol solvated complex, after desolvating, raises new questions however.

Experimental Section

The complexes were prepared as described[14,15] by Sorai et al. The syntheses were carried out by using Schlenk apparatus, and the recrystallizations and all product handling were carried out in a dry nitrogen atmosphere. The desolvated complex $[Fe(\alpha\text{-P})_3]Br_2$ was prepared by pumping the ethanol solvated complex $[Fe(\alpha\text{-P})_3]Br_2\cdot C_2H_5OH$ on a high-vacuum line at 80 °C for 24 h. Magnetic susceptibilities and moments were determined by using a superconducting susceptometer incorporating a Josephson junction magnetometer, superconducting magnets, and shields.[7]

Crystal data for $[Fe(\alpha\text{-P})_3]Cl_2\cdot C_2H_5OH$: $FeCl_2O_2N_6C_{20}H_{30}$; mol wt 493; space group $P2_1/c$; $Z = 4$; $a = 10.937$ (5), $b = 22.061$ (9), $c = 11.571$ (6) Å; $\beta = 116.70$ (4)°; $V = 2496$ Å^3; $\rho_{calcd} = 1.31$, $\rho_{obsd} = 1.30$ g cm^{-3}; μ(Mo Kα) = 8.6 cm^{-1}; crystal dimensions (in mm from centroid) (100) 0.05, ($\bar{1}$00) 0.05, (010) 0.15, (0$\bar{1}$0) 0.15, (001) 0.15, (00$\bar{1}$) 0.15; maximum and minimum transmission coefficients = 0.95, 0.92.

The crystal was mounted in a glass capillary in a nitrogen atmosphere to protect it from oxygen and water. The Enraf-Nonius program SEARCH was used to obtain 25 accurately centered reflections which were then used in the program INDEX to obtain approximate

0020-1669/79/1318-2692$01.00/0

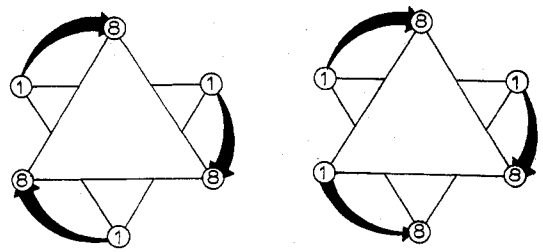

A B

Figure 1. Configuration of the $[Fe(\alpha\text{-}P)_3]^{2+}$ ion in (A) $[Fe(\alpha\text{-}P)_3]Cl_2\cdot 2H_2O$ and (B) $[Fe(\alpha\text{-}P)_3]Cl_2\cdot S$ (S = CH_3OH, C_2H_5OH).

cell dimensions and an orientation matrix for data collection. Refined cell dimensions and their estimated standard deviations were obtained from the least-squares refinement of 25 accurately centered reflections. The mosaicity of the crystal was examined by the ω-scan technique and judged to be satisfactory.

Collection and Reduction of Data. Diffraction data were collected at 292 K on an Enraf-Nonius four-circle CAD-4 diffractometer controlled by a PDP8/M computer using Mo Kα radiation from a highly oriented graphite crystal monochromator. The θ–2θ scan technique was used to record the intensities for all nonequivalent reflections for which $1° < 2\theta < 45°$. Scan widths (SW) were calculated from the formula $SW = A + B \tan\theta$ where A is estimated from the mosaicity of the crystal and B allows for the increase in peak width due to $K\alpha_1$–$K\alpha_2$ splitting. The values of A and B were 0.7 and 0.35°, respectively. The calculated scan angle is extended at each side by 25% for background determination (BG1 and BG2). The net count is then calculated as NC = TOT − 2(BG1 + BG2) where TOT is the integrated peak intensity. Reflection data were considered insignificant if intensities registered less than 10 counts above background on a rapid prescan, such reflections being rejected automatically by the computer.

The intensities of four standard reflections, monitored at 100 reflection intervals, showed no greater fluctuations during the data collection than those expected from Poisson statistics. The raw intensity data were corrected for Lorentz–polarization effects (including the polarization effect of the crystal monochromator) and then for absorption. Of the 2867 independent intensities, 1470 had $F_o^2 > 3\sigma(F_o^2)$, where $\sigma(F_o^2)$ was estimated from counting statistics.[16] These data were used in the final refinement of the structural parameters.

Determination and Refinement of the Structure. The position of the metal atom was determined from a three-dimensional Patterson function calculated from all the intensity data. The intensity data were phased sufficiently well by these positional coordinates to permit location of the remaining nonhydrogen and some of the hydrogen atoms.

Full-matrix least-squares refinement was based on F, and the function minimized was $\sum w(|F_o| - |F_c|)^2$. The weights w were then taken as $[2F_o/\sigma(F_o^2)]^2$, where $|F_o|$ and $|F_c|$ are the observed and calculated structure factor amplitudes. The atomic scattering factors for nonhydrogen atoms were taken from Cromer and Waber[17] and those for hydrogen from Stewart et al.[18] The effects of anomalous dispersion for all nonhydrogen atoms were included in F_c by using the values of Cromer and Ibers[19] for $\Delta f'$ and $\Delta f''$. Agreement factors are defined as $R = \sum||F_o| - |F_c||/\sum|F_o|$ and $R_w = (\sum w(|F_o| - |F_c|)^2/\sum w|F_o|^2)^{1/2}$.

Anisotropic temperature factors were introduced for all nonhydrogen atoms. Further Fourier difference functions permitted location of the remaining hydrogen atoms. The hydrogen atoms were included in the refinement for three cycles of least-squares refinement and subsequently held fixed. The models converged with $R = 5.3\%$ and $R_w = 6.1\%$. A final Fourier difference function was featureless. Tables of the observed and calculated structure factors are available.[20] The principal programs used are as previously described.[21]

Results and Discussion

Final positional and thermal parameters for $[Fe(\alpha\text{-}P)_3]Cl_2\cdot C_2H_5OH$ are given in Table I. Tables II and III contain the bond lengths and angles. The digits in parentheses in the tables are the estimated standard deviations in the least significant figures quoted and were derived from the inverse

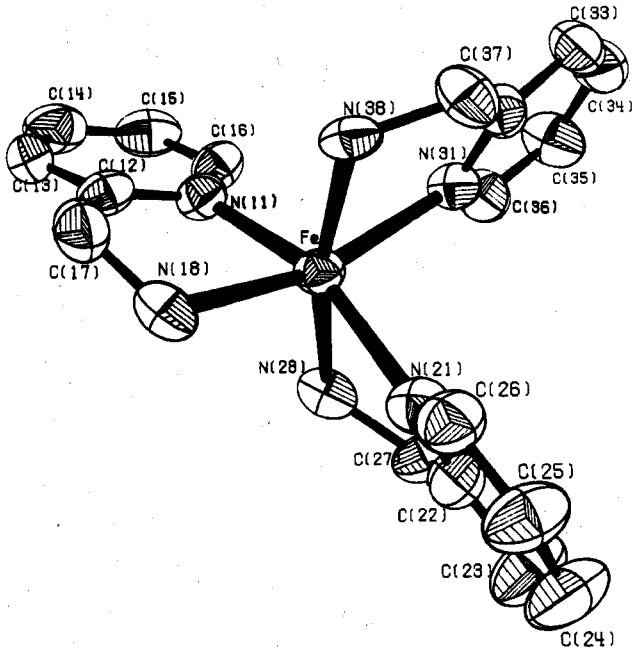

Figure 2. ORTEP diagram of $[Fe(\alpha\text{-}P)_3]^{2+}$ in $[Fe(\alpha\text{-}P)_3]Cl_2\cdot C_2H_5OH$.

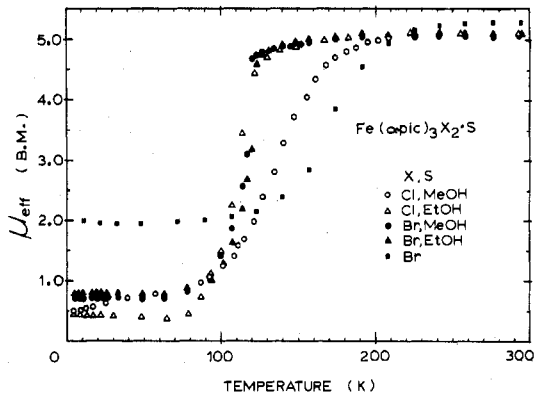

Figure 3. Observed magnetic moments μ (μ_B) for $[B]X_2\cdot S$ (X = Cl, Br; S = CH_3OH, C_2H_5OH, nothing).

matrix in the course of least-squares refinement calculations. Figure 2 shows the $[Fe(\alpha\text{-}P)_3]^{2+}$ ion as it exists in this complex. This cation is clearly of form B as in the methanol analogue.[12]

Despite the different space groups, there is close similarity between $[B]Cl_2\cdot C_2H_5OH$ ($P2_1/c$) and the known structure of $[B]Cl_2\cdot CH_3OH$ ($Pbcn$)[12] in several important respects. Solvent to cation hydrogen bonds are entirely absent, unlike the case of $[A]Cl_2\cdot 2H_2O$, where such bonding is extensive.[12] There is merely a hydroxyl–chloride link. The halogen to cation contacts via ligand amino nitrogen atoms are very similar in both compounds, forming a two-dimensional network in each case. The average metal–ligand bond distance is much longer in the ethanol solvate than in $[A]Cl_2\cdot 2H_2O$, leading to a 0.18 Å difference between the high-spin B and low-spin A cations.

The magnetic properties of $[B]Cl_2\cdot C_2H_5OH$, $[Fe(\alpha\text{-}P)_3Br_2\cdot CH_3OH$, and $[Fe(\alpha\text{-}P)_3]Br_2\cdot C_2H_5OH$ are shown in Figure 3, together with the literature data[12] for the $[B]Cl_2\cdot CH_3OH$ complex. Also shown is the temperature dependence of the magnetic moment of the desolvated complex $[Fe(\alpha\text{-}P)_3]Br_2$, formed by removal of the ethanol of crystallization from $[Fe(\alpha\text{-}P)_3]Br_2\cdot C_2H_5OH$. In each case there is a strong temperature dependence of the magnetic moment. Each of the complexes $[Fe(\alpha\text{-}P)_3]Br_2\cdot CH_3OH$, $[Fe(\alpha\text{-}P)_3]Br_2\cdot C_2H_5OH$, and $[B]Cl_2\cdot C_2H_5OH$ is high spin at room temperature and each undergoes a similar transition to low spin in the region 130–90 K. In each case the transition is

Table I. Positional and Thermal Parameters and Their Estimated Standard Deviations[a]

atom	x	y	z	U_{11}	U_{22}	U_{33}	U_{12}	U_{13}	U_{23}
Fe	0.0280 (2)	0.13411 (7)	0.3054 (1)	0.0701 (8)	0.0312 (8)	0.0451 (6)	0.0021 (9)	0.0394 (5)	0.0032 (8)
Cl(1)	0.1353 (3)	0.5688 (1)	−0.0622 (2)	0.086 (2)	0.044 (2)	0.057 (1)	−0.010 (1)	0.052 (1)	−0.007 (1)
Cl(2)	0.2475 (3)	0.2733 (1)	0.5699 (3)	0.103 (2)	0.055 (2)	0.097 (2)	−0.013 (2)	0.075 (1)	−0.018 (2)
O	0.336 (1)	0.3871 (5)	0.459 (2)	0.25 (1)	0.087 (9)	0.40 (2)	0.032 (8)	0.200 (8)	0.060 (9)
N(11)	0.2363 (8)	0.1036 (4)	0.3714 (8)	0.054 (5)	0.042 (5)	0.062 (5)	−0.009 (5)	0.034 (3)	−0.014 (5)
N(18)	0.1046 (8)	0.1372 (4)	0.5109 (8)	0.067 (5)	0.038 (5)	0.079 (5)	−0.007 (5)	0.054 (3)	−0.006 (5)
N(21)	−0.1478 (8)	0.1946 (4)	0.2699 (8)	0.064 (5)	0.030 (5)	0.072 (5)	0.013 (4)	0.050 (3)	0.016 (4)
N(28)	0.0845 (8)	0.2230 (4)	0.2606 (8)	0.032 (5)	0.044 (5)	0.030 (5)	−0.011 (5)	−0.001 (4)	−0.004 (4)
N(31)	−0.0533 (9)	0.0983 (4)	0.1073 (7)	0.088 (5)	0.044 (5)	0.044 (4)	0.001 (5)	0.048 (3)	0.008 (4)
N(38)	−0.0649 (8)	0.0482 (4)	0.3155 (7)	0.086 (6)	0.030 (5)	0.022 (4)	0.004 (5)	0.029 (3)	−0.003 (4)
C(12)	0.309 (1)	0.0931 (5)	0.5020 (10)	0.021 (7)	0.035 (7)	0.056 (7)	−0.002 (6)	−0.002 (5)	−0.009 (6)
C(13)	0.438 (1)	0.0781 (6)	0.5605 (12)	0.067 (9)	0.050 (8)	0.085 (9)	0.010 (7)	0.016 (6)	−0.000 (7)
C(14)	0.514 (1)	0.0752 (6)	0.4904 (15)	0.038 (8)	0.050 (8)	0.151 (11)	0.008 (7)	0.028 (7)	0.009 (9)
C(15)	0.453 (1)	0.0889 (5)	0.3673 (13)	0.087 (7)	0.044 (8)	0.144 (9)	0.031 (6)	0.078 (5)	0.025 (7)
C(16)	0.317 (1)	0.1021 (5)	0.3081 (11)	0.143 (9)	0.035 (7)	0.097 (7)	0.023 (7)	0.085 (5)	0.023 (6)
C(17)	0.223 (1)	0.0945 (6)	0.5757 (10)	0.070 (7)	0.064 (8)	0.060 (6)	−0.009 (7)	0.040 (4)	0.000 (6)
C(22)	−0.155 (1)	0.2467 (5)	0.2042 (10)	0.062 (6)	0.034 (6)	0.076 (6)	0.002 (6)	0.050 (4)	0.005 (6)
C(23)	−0.260 (1)	0.2861 (5)	0.1686 (11)	0.090 (7)	0.044 (7)	0.077 (7)	0.023 (6)	0.054 (5)	0.023 (6)
C(24)	−0.368 (1)	0.2729 (5)	0.1946 (12)	0.085 (8)	0.052 (8)	0.103 (8)	0.037 (6)	0.056 (5)	0.022 (7)
C(25)	−0.365 (1)	0.2194 (5)	0.2603 (12)	0.067 (7)	0.051 (8)	0.097 (8)	0.018 (6)	0.048 (5)	0.010 (7)
C(26)	−0.256 (1)	0.1827 (5)	0.2941 (11)	0.120 (7)	0.031 (7)	0.112 (7)	0.010 (6)	0.092 (4)	0.014 (6)
C(27)	−0.035 (1)	0.2579 (5)	0.1766 (10)	0.104 (7)	0.031 (6)	0.083 (6)	0.008 (6)	0.068 (4)	0.024 (6)
C(32)	−0.144 (1)	0.0494 (5)	0.0765 (9)	0.071 (7)	0.055 (7)	0.035 (5)	0.005 (6)	0.030 (4)	0.010 (6)
C(33)	−0.195 (1)	0.0222 (6)	−0.0402 (10)	0.085 (8)	0.069 (9)	0.042 (6)	−0.021 (7)	0.033 (5)	−0.009 (6)
C(34)	−0.168 (1)	0.0419 (6)	−0.1378 (10)	0.083 (9)	0.071 (9)	0.037 (6)	−0.002 (8)	0.020 (5)	−0.011 (6)
C(35)	−0.081 (1)	0.0898 (5)	−0.1109 (9)	0.106 (8)	0.059 (8)	0.027 (5)	−0.002 (7)	0.037 (5)	−0.001 (6)
C(36)	−0.029 (1)	0.1177 (5)	0.0072 (11)	0.077 (8)	0.041 (7)	0.062 (6)	0.003 (6)	0.037 (5)	0.003 (6)
C(37)	−0.172 (1)	0.0313 (5)	0.1899 (9)	0.034 (6)	0.057 (8)	0.052 (6)	0.005 (6)	0.023 (4)	0.015 (6)
C(1)	0.473 (2)	0.3853 (10)	0.4737 (23)	0.078 (13)	0.207 (21)	0.222 (22)	0.001 (15)	0.014 (13)	0.049 (18)
C(2)	0.497 (2)	0.3355 (8)	0.4199 (15)	0.387 (17)	0.170 (14)	0.117 (10)	0.178 (12)	0.158 (9)	0.084 (10)

atom	x	y	z	B, Å^2	atom	x	y	z	B, Å^2
H(13)	0.49 (1)	0.074 (5)	0.65 (1)	3 (3)	H(272)	−0.07 (1)	0.249 (5)	0.08 (1)	4 (3)
H(14)	0.62 (1)	0.067 (5)	0.54 (1)	5 (3)	H(281)	0.14 (1)	0.244 (5)	0.34 (1)	8 (3)
H(15)	0.51 (1)	0.089 (5)	0.33 (1)	6 (3)	H(282)	0.14 (1)	0.222 (5)	0.23 (1)	7 (3)
H(16)	0.26 (1)	0.109 (5)	0.21 (1)	6 (3)	H(33)	−0.26 (1)	−0.013 (5)	−0.06 (1)	5 (3)
H(171)	0.28 (1)	0.104 (5)	0.67 (1)	9 (3)	H(34)	−0.20 (1)	0.022 (5)	−0.22 (1)	4 (3)
H(172)	0.19 (1)	0.055 (5)	0.58 (1)	5 (3)	H(35)	−0.05 (1)	0.102 (5)	−0.17 (1)	6 (3)
H(181)	0.13 (1)	0.177 (5)	0.54 (1)	6 (3)	H(36)	0.03 (1)	0.152 (5)	0.04 (1)	6 (3)
H(182)	0.04 (1)	0.130 (5)	0.53 (1)	4 (3)	H(371)	−0.20 (1)	−0.015 (5)	0.17 (1)	5 (3)
H(23)	−0.26 (1)	0.319 (5)	0.13 (1)	6 (3)	H(372)	−0.27 (1)	0.047 (5)	0.16 (1)	6 (3)
H(24)	−0.46 (1)	0.297 (5)	0.16 (1)	5 (3)	H(381)	−0.02 (1)	0.017 (5)	0.32 (1)	−0 (3)
H(25)	−0.45 (1)	0.207 (5)	0.27 (1)	7 (3)	H(382)	−0.10 (1)	0.050 (5)	0.37 (1)	5 (3)
H(26)	−0.26 (1)	0.147 (5)	0.34 (1)	4 (3)	H	0.27 (0)	0.350 (0)	0.38 (0)	6 (0)
H(271)	−0.01 (1)	0.299 (5)	0.19 (1)	4 (3)					

[a] The expression for the temperature factors has the form $\exp(-T)$ where $T = 8\pi^2 U(\sin^2\theta)/\lambda^2$ for isotropic atoms and $T = 2\pi^2 \Sigma h_i h_j U_{ij} a_i^* a_j^*$ for anisotropic atoms.

Table II

Bond Lengths and Closest Intermolecular Contacts (Å)

Fe-N(11)	2.159 (7)	N(21)-C(22)	1.362 (9)	C(12)-C(13)	1.308 (12)	C(25)-C(26)	1.344 (11)
Fe-N(18)	2.140 (7)	N(21)-C(26)	1.362 (10)	C(12)-C(17)	1.528 (11)	C(32)-C(33)	1.350 (10)
Fe-N(21)	2.222 (6)	N(28)-C(27)	1.453 (9)	C(13)-C(14)	1.396 (14)	C(32)-C(37)	1.532 (10)
Fe-N(28)	2.187 (6)	N(31)-C(32)	1.396 (9)	C(14)-C(15)	1.309 (15)	C(33)-C(34)	1.360 (11)
Fe-N(31)	2.202 (7)	N(31)-C(36)	1.367 (9)	C(15)-C(16)	1.360 (14)	C(34)-C(35)	1.360 (11)
Fe-N(38)	2.179 (6)	N(38)-C(37)	1.448 (9)	C(22)-C(23)	1.351 (10)	C(35)-C(36)	1.368 (11)
N(11)-C(12)	1.375 (10)	⟨N-H⟩	0.90	C(22)-C(27)	1.501 (10)	O-C(1)	1.429 (16)
N(11)-C(16)	1.378 (11)	⟨C-H⟩	0.98	C(23)-C(24)	1.374 (11)	C(1)-C(2)	1.341 (21)
N(18)-C(17)	1.502 (10)	O-H	1.19	C(24)-C(25)	1.397 (11)		

H-Bonding Contacts

C_2H_5OH complex						CH_3OH complex					
Cl-	d_1	-H-	d_2	-N	d(Cl-N)	Cl-	d_1	-H-	d_2	-N	d(Cl-N)
(2)	2.406	(181)	0.938	(18)	3.31	(1)	2.469	(181)	0.895	(18)	3.33
(1)	2.527	(182)	0.825	(18)	3.30	(2)	2.330	(182)	0.937	(18)	3.25
(2)	2.464	(281)	0.971	(28)	3.39	(2)	2.445	(281)	0.982	(28)	3.41
(2)	2.603	(282)	0.821	(28)	3.41	(2)	2.491	(282)	0.932	(28)	3.40
(1)	2.503	(381)	0.853	(38)	3.27	(1)	2.549	(381)	0.780	(38)	3.31
(1)	2.437	(382)	0.901	(38)	3.31	(1)	2.316	(382)	1.026	(38)	3.28

relatively sharp, being mostly complete in the region 130–110 K, and is sharper than in the analogous complex $[B]Cl_2 \cdot CH_3OH$. The maximum change in magnetic moment occurs at 120, 123, and 117 K for $[Fe(\alpha\text{-}P)_3]Br_2 \cdot CH_3OH$, $[Fe(\alpha\text{-}P)_3]Br_2 \cdot C_2H_5OH$, and $[B]Cl_2 \cdot C_2H_5OH$, respectively. The similarity of the magnetic behavior is good evidence for the

Table III. Bond Angles (deg)

N(11)-Fe-N(18)	78.0 (3)	C(32)-N(31)-C(36)	114.1 (7)
N(11)-Fe-N(21)	160.1 (2)	Fe-N(38)-C(37)	110.9 (4)
N(11)-Fe-N(28)	89.9 (2)	N(11)-C(12)-C(13)	124.6 (9)
N(11)-Fe-N(31)	97.2 (3)	N(11)-C(12)-C(17)	114.5 (8)
N(11)-Fe-N(38)	98.8 (2)	C(13)-C(12)-C(17)	120.6 (5)
N(18)-Fe-N(21)	93.4 (3)	C(12)-C(13)-C(14)	119.7 (5)
N(18)-Fe-N(28)	103.0 (2)	C(13)-C(14)-C(15)	118.6 (5)
N(18)-Fe-N(31)	160.7 (2)	C(14)-C(15)-C(16)	120.3 (5)
N(18)-Fe-N(38)	85.8 (2)	N(11)-C(16)-C(15)	123.6 (5)
N(21)-Fe-N(28)	74.4 (2)	N(18)-C(17)-C(12)	109.9 (7)
N(21)-Fe-N(31)	96.4 (3)	N(21)-C(22)-C(23)	122.8 (8)
N(21)-Fe-N(38)	98.4 (2)	N(21)-C(22)-C(27)	114.9 (7)
N(28)-Fe-N(31)	95.7 (2)	C(23)-C(22)-C(27)	122.3 (8)
N(28)-Fe-N(38)	168.8 (2)	C(22)-C(23)-C(24)	119.7 (8)
N(31)-Fe-N(38)	76.3 (2)	C(23)-C(24)-C(25)	119.1 (8)
Fe-N(11)-C(12)	116.0 (6)	C(24)-C(25)-C(26)	118.1 (8)
Fe-N(11)-C(16)	130.2 (8)	N(21)-C(26)-C(25)	124.2 (8)
C(12)-N(11)-C(16)	112.9 (8)	N(28)-C(27)-C(22)	112.4 (7)
Fe-N(18)-C(17)	110.8 (4)	N(31)-C(32)-C(33)	121.8 (7)
Fe-N(21)-C(22)	116.0 (5)	N(31)-C(32)-C(37)	112.1 (7)
Fe-N(21)-C(26)	127.5 (5)	C(33)-C(32)-C(37)	126.1 (9)
C(22)-N(21)-C(26)	116.2 (7)	C(32)-C(33)-C(34)	122.8 (8)
Fe-N(28)-C(27)	111.6 (4)	C(33)-C(34)-C(35)	116.5 (8)
Fe-N(31)-C(32)	116.8 (5)	C(34)-C(35)-C(36)	120.8 (8)
Fe-N(31)-C(36)	129.0 (6)	N(31)-C(36)-C(35)	123.7 (8)
O-C(1)-C(2)	112.3 (5)	N(38)-C(37)-C(32)	114.2 (7)

same structure, B, of the cations in all three complexes.

Removal of the solvent molecule from $[B]Br_2 \cdot C_2H_5OH$ has a dramatic effect on the magnetism. Instead of the sharp rise from low spin to high spin in each of the solvated complexes, there is a very gradual decrease in magnetic moment with lowering temperature, but the low-spin value is not even approached (Figure 3). Although there is still a spin-state equilibrium in the desolvated complex, it is no longer obvious what species are involved. Clearly, the high-spin form is present at high temperatures, but a permanently paramagnetic material persists at low temperature. Whether this consists of a mixture of high-spin and diamagnetic low-spin iron(II) complexes or whether an intermediate spin state is present is not certain. Further work is in progress on this point and on the reason for the somewhat sharper transition in $[B]Br_2 \cdot S$ (S = CH_3OH, C_2H_5OH) and $[B]Cl_2 \cdot C_2H_5OH$, but it is already possible to explain the apprently anomalous literature results[13] on these complexes. The varying types of spin-state high-spin to low-spin transitions reported for these complexes depend on the degree of drying to which they were subjected. The very gradual transition reported for the bromide complex thus represents such a dried material. The sharp transitions observed in the methanol and ethanol solvates of the bromide complex show that the Br^- anion does not behave differently from the Cl^- anion when the two complexes are similarly handled. The differences reported in the literature were therefore merely solvent effects, not due to differences in the two halogens.

Some structural and magnetic features of the compounds can be correlated with each other. The pure low-spin $[A]Cl_2 \cdot 2H_2O$ complex has all three amino nitrogen ligands cis on one triangular face of an octahedron, where they are hydrogen bonded to the water molecules. This reduces the amount of chloride to amine nitrogen contact, compared with the ethanol and methanol solvates which have no cation to solvent hydrogen bonding. Possibly the close approach of the halogen ions (observed in the $[Fe(\alpha\text{-}P)_3]Cl_2 \cdot S$ complexes and surmised in the $[Fe(\alpha\text{-}P)_3]Br_2 \cdot S$ complexes) to the amino nitrogens causes a slight weakening of the Fe–N bonds, thus making it easier to attain a high-spin configuration at high temperatures. Another possibility is that the more distorted form of the cation, B, tends to favor high spin more than A. There is some support for this in the observation that removal of ethanol from a complex containing B leaves a room-temperature high-spin species while removal of water from a complex containing A does not increase the magnetism enough to produce high spin.[22] A specific question that remains to be answered is whether the process of solvent removal can reverse a ligand and thereby convert the cation from form A to form B and vice versa, and since the solvent is involved in hydrogen bonding in the lattice, such a possibility cannot be ruled out completely, although it does appear unlikely.

The low-temperature properties of the desolvated complex $[Fe(\alpha\text{-}P)_3]Br_2$ prepared from $[Fe(\alpha\text{-}P)_3]Br_2 \cdot C_2H_5OH$ are more mysterious. They conform to the properties of neither of the two possible cations A or B, as observed in the complexes $[Fe(\alpha\text{-}P)_3]X_2 \cdot S$ (X = Cl, Br; S = $2H_2O$, ethanol, methanol), and can therefore not be explained in terms of the properties observed for the solvates. The problem is the currently incomplete knowledge of how either of the cations A or B behaves when no solvent is present in the lattice and whether the properties of either form are affected by its previous history. A Mössbauer study will readily determine whether the intermediate moment, which is somewhat low for an $S = 1$ state in the low-temperature region, for the desolvated bromide complex is due to a physical mixture or a single species and therefore a single spin state.

The bromide complexes, and presumably also the chloride analogues, show a marked thermochromic effect concomitant with the change in electronic ground state from high spin (green) to low spin (solvated, dark brown; unsolvated, red-brown). Spectral investigation of the thermochromic effect in the crossover region should provide a great deal of information on the electronic structure of the two spin states and possibly provide information on the mechanism of spin crossover.

Acknowledgment. Support received under NSF Grant CHE77-01372 is gratefully acknowledged.

Registry No. $[Fe(\alpha\text{-}P)_3]Cl_2 \cdot C_2H_5OH$, 71097-03-5; $[Fe(\alpha\text{-}P)_3]Br_2$, 71097-04-6.

Supplementary Material Available: A listing of structure factor amplitudes (7 pages). Ordering information is given on any current masthead page.

References and Notes

(1) Ewald, A. H.; Martin, R. L.; Sinn, E.; White, A. H. *Inorg. Chem.* **1969**, *8*, 1837.
(2) Harris, C. M.; Lockyer, T. N.; Martin, R. L.; Patil, H. R. H.; Sinn, E.; Stewart, I. M. *Aust. J. Chem.* **1969**, *22*, 2105.
(3) Sylva, R. N.; Goodwin, H. A. *Aust. J. Chem.* **1967**, *20*, 479.
(4) Harris, C. M.; Sinn, E. *Inorg. Chim. Acta* **1967**, *2*, 296.
(5) Butcher, R. J.; Sinn, E. *J. Am. Chem. Soc.* **1976**, *98*, 2440.
(6) Butcher, R. J.; Sinn, E. *J. Am. Chem. Soc.*, **1976**, *98*, 5159.
(7) Cukauskas, E. J.; Deaver, B. S.; Sinn, E. *J. Chem. Phys.* **1977**, *67*, 1257.
(8) Cukauskas, E. J.; Deaver, B. S.; Sinn, E. *Inorg. Nucl. Chem. Lett.* **1977**, *13*, 283.
(9) Sinn, E.; Sim, P. G.; Dose, E. V.; Tweedle, M. F.; Wilson, L. J. *J. Am. Chem. Soc.* **1978**, *100*, 3375.
(10) Tweedle, M. F.; Wilson, L. J. *J. Am. Chem. Soc.* **1976**, *98*, 4824.
(11) Mitra, S.; White, A. H.; Raston, C. L. *Aust. J. Chem.* **1976**, *29*, 1897.
(12) Greenaway, A. M.; Sinn, E. *J. Am. Chem. Soc.* **1978**, *100*, 8080.
(13) Renovitch, G. A.; Baker, W. A. *J. Am. Chem. Soc.* **1967**, *89*, 6377.
(14) Sorai, M.; Ensling, J.; Gütlich, P. *Chem. Phys.* **1976**, *18*, 199.
(15) Sorai, M.; Ensling, J.; Hasselbach, K. M.; Gütlich, P. *Chem. Phys.* **1977**, *20*, 197.
(16) Corfield, P. W. R.; Doedens, R. J.; Ibers, J. A. *Inorg. Chem.* **1967**, *6*, 197.
(17) Cromer, D. T.; Waber, J. T. "International Tables for X-ray Crystallography;" Kynoch Press: Birmingham, England, 1974; Vol. IV.
(18) Stewart, R. F.; Davidson, E. R.; Simpson, W. T. *J. Chem. Phys.* **1965**, *42*, 3175.
(19) Cromer, D. T.; Ibers, J. A., ref 17.
(20) Supplementary material.
(21) Freyberg, D. P.; Mockler, G. M.; Sinn, E., *J. Chem. Soc., Dalton Trans.* **1976**, 447.
(22) Greenaway, A. M.; O'Connor, C. J.; Sinn, E., unpublished work.